Psychiatry Research: Neuroimaging 173 (2009) 8–14

Contents lists available at ScienceDirect

Psychiatry Research: Neuroimaging

journal homepage: www.elsevier.com/locate/psychresns

# Principal component analysis in mild and moderate Alzheimer's disease — A novel approach to clinical diagnosis

Marco Pagani[a,b,*], Dario Salmaso[a], Guido Rodriguez[c], Davide Nardo[d], Flavio Nobili[c]

[a]Institute of Cognitive Sciences and Technologies, CNR, Rome & Padua, Italy
[b]Department of Nuclear Medicine, Karolinska Hospital, Stockholm, Sweden
[c]Clinical Neurophysiology, Departmentt of Endocrinological and Medical Sciences, S. Martino Hospital and University of Genoa, Italy
[d]Department of Neuroscience, AFaR, Ospedale Fatebenefratelli, Rome, Italy

ARTICLE INFO

*Article history:*
Received 14 June 2007
Received in revised form 11 July 2008
Accepted 11 July 2008

*Keywords:*
Computerised Brain Atlas
Dementia
Discriminant analysis
SPECT
Volume of interest analysis

ABSTRACT

Principal component analysis (PCA) provides a method to explore functional brain connectivity. The aim of this study was to identify regional cerebral blood flow (rCBF) distribution differences between Alzheimer's disease (AD) patients and controls (CTR) by means of volume of interest (VOI) analysis and PCA. Thirty-seven CTR, 30 mild AD (mildAD) and 27 moderate AD (modAD) subjects were investigated using single photon emission computed tomography with $^{99m}$Tc-hexamethylpropylene amine oxime. Analysis of covariance (ANCOVA), PCA, and discriminant analysis (DA) were performed on 54 VOIs. VOI analysis identified in both mildAD and modAD subjects a decreased rCBF in six regions. PCA in mildAD subjects identified four principal components (PCs) in which the correlated VOIs showed a decreased level of rCBF, including regions that are typically affected early in the disease. In five PCs, including parietal-temporal-limbic cortex, and hippocampus, a significantly lower rCBF in correlated VOIs was found in modAD subjects. DA significantly discriminated the groups. The percentage of subjects correctly classified was 95, 70, and 81 for CTR, mildAD and modAD groups, respectively. PCA highlighted, in mildAD and modAD, relationships not evident when brain regions are considered as independent of each other, and it was effective in discriminating groups. These findings may allow neurophysiological inferences to be drawn regarding brain functional connectivity in AD that might not be possible with univariate analysis.



## 1. Introduction

Comparisons between regional cerebral blood flow (rCBF) patterns in Alzheimer's disease (AD) patients and normal controls (CTR) by single photon emission computed tomography (SPECT) or positron emission tomography (PET) have in the past mainly been carried out by either visual evaluation or outlining the regions of interest (ROIs) in a manual or semiautomatic mode (Syed et al., 1992; Salmon et al., 1994; Bonte et al., 1997; Jagust et al., 1997, 2001). In recent years, several digitized spatial standardization software programs have been introduced, and some of them have been extensively used both in research and clinical investigations (Friston et al., 1995; Worsley et al., 1996; Hirsch et al., 1997; Houston et al., 1998; Bartenstein et al., 1997; Imran et al., 1999). Among them, the Computerized Brain Atlas (CBA) (Greitz et al., 1991; Thurfjell et al., 1995; Andersson and Thurfjell, 1997), when registered to imaging data, defines volumes of interest (VOIs), corresponding to anatomical and functional areas of the brain (Brodmann areas and deep grey structures). It thus allows investigating rCBF relationships between anatomically distributed but physiologically correlated brain regions using principal component analysis (PCA) (Pagani et al., 2002). Moreover, the univariate approach treats all variables as if they represent independent measures across brain regions, thus ignoring the extensive and structured connections between them. Possible networking is better investigated by multivariate analysis describing pattern of covariance at both the voxel and VOI levels.

Multivariate spatial covariance methods have been proposed in functional neuroimaging by several authors (Moeller et al., 1987, 1999; Eidelberg et al., 1990, 1994; Friston et al., 1993, 1999; Strother et al., 1995; McIntosh et al., 1996; Jones et al., 1998; Zuendorf et al., 2003; Greicius et al., 2004; Lozza et al., 2004; Habeck et al., 2005; Hu et al., 2005; Kerrouche et al., 2006). All such studies were meant to overcome the concept of functional segregation as derived by univariate analysis of independent variables and to interpret the results in the frame of knowledge of brain circuitry and thus from a more holistic point of view.

The application of PCA aims to reduce the dimensionality of the data matrix through the grouping of VOIs into principal components that will undergo further statistical analysis. In AD, the rCBF

* Corresponding author. Institute of Cognitive Sciences and Technologies, CNR Via S. Martino della Battaglia 44, 00185 Rome, Italy. Tel.: +39 06 44595321; fax: +39 06 44595243.
*E-mail address:* marco.pagani@istc.cnr.it (M. Pagani).

0925-4927/$ – see front matter © 2008 Elsevier Ireland Ltd. All rights reserved.
doi:10.1016/j.pscychresns.2008.07.016

distribution is likely to be the result of a combination of pathological lesions and the effects they can have on distant parts of the brain (Stoub et al., 2006). Such an approach has been applied to $^{18}$F-FDG PET data to characterize patterns of covariance in AD (Salmon et al., 2007) and to distinguishing between AD and vascular dementia (VaD) (Kerrouche et al., 2006). In studies of resting state rCBF with $H_2^{15}O$ PET (Scarmeas et al., 2004; Devanand et al., 2006) or SPECT (Huang et al., 2007), AD patients and subjects with mild cognitive impairment showed a distinct covariance pattern versus controls. PCA has been successfully performed implementing both a voxel-based analysis (Kerrouche et al., 2006; Scarmeas et al., 2004; Devanand et al., 2006) and using discrete regions of interest (Huang et al., 2007). These studies have consistently shown that PC composition may allow inferences on the peculiar functional re-organization of brain networking in both AD dementia and pre-dementia states, as well as in VaD (Kerrouche et al., 2006) and frontotemporal dementia (Salmon et al., 2006). Therefore, we hypothesised that investigating AD by means of multivariate analysis (i.e. PCA) might add knowledge about the rCBF pattern and neural connectivity underlying this complex neurodegenerative disorder.

The aim of the present study is to use multivariate statistical methodology to assess rCBF distribution differences between two groups of AD patients with different levels of disease severity and a group of normal controls.

## 2. Methods

### 2.1. Participants

#### 2.1.1. Normal subjects

About 100 subjects older than 50 years were contacted by the Unit of Clinical Neurophysiology of the University of Genoa during University courses reserved for elderly people. Forty-four subjects agreed to participate and underwent brain SPECT examination by the same procedure used for patients. All subjects were carefully screened by general medical history and clinical examination. Complete blood counts, serum glucose, creatinine and total cholesterol, blood urea nitrogen, and urinalysis were performed, and the results had to be normal for the subjects to be enrolled in the control group. Previous or present neurological, psychiatric, metabolic or cardiovascular disorders and current medication of any kind were the other exclusion criteria. The Mini-Mental State Examination (MMSE) (Folstein et al., 1975) was performed and only subjects with a normal score were considered. Thirty-seven subjects (14 males and 23 females, ranging in age from 52 to 78 years; mean: 63.8 ± 7.6) matched these requisites and formed the control group (CTR). All subjects were informed about the study procedures and gave their consent to participate.

#### 2.1.2. Patients

Over a 3-year period, all of the consecutive outpatients with probable AD (according to the definition of the NINCDS-ADRDA work group) (McKhann et al., 1984) in the mild or moderate stage of the disease (i.e., scoring 9 or higher on the MMSE) who came to the Clinical Neurophysiology Unit of the University of Genoa for a first diagnostic evaluation were considered eligible for this study.

All of the patients underwent a complete diagnostic work-up according to current standards, which include general and neurological examinations, a standardized neuropsychological assessment, basal computed tomography or magnetic resonance imaging and other routine blood and urine screening investigations to rule out secondary dementias. The presence of previous or present major psychiatric disorders, serious neurological diseases, severe and uncontrolled arterial hypertension, diabetes mellitus, renal, hepatic or respiratory failure, anemia (Hb level<10 mg/dl) or malignancies constituted exclusion criteria. In conformity with the diagnosis of AD, all patients scored lower than 4 on the Hachinski ischaemic scale. Lewy-body dementia, frontotemporal dementia and vascular dementia were excluded in all patients on the basis of current clinical criteria (Roman et al., 1993; The Lund and Manchester Groups, 1994; McKeith et al., 1999).

All patients underwent brain perfusion SPECT examination as part of the routine diagnostic procedure. The study population included 57 patients (37 women and 20 men), aged 55 to 89 years (mean 71.9 ± 7.0), with years of full education ranging from 3 to 17 (mean: 7.2 ± 4.2). The MMSE score ranged from 9 to 28 (mean 19.4 ± 5.5). All of the patients were undergoing their first diagnostic evaluation for cognitive complaints, and thus none of them were being treated with acetylcholinesterase inhibitors or with other neuropsychoactive drugs. The patients (or their relatives) were informed about the finalities of the study and gave their informed consent. On the basis of the MMSE score, this patient population was divided into two groups. The first group included 27 patients (8 males and 19 females, mean age: 72.3 ± 7.4) with a MMSE score <20 (mean: 14.6 ± 3.5) (modAD). The second group included 30 patients (12 males and 18 females, mean age: 71.7 ± 6.9) with a MMSE score >20 (mean: 23.7 ± 2.3) (mildAD). The study was approved by the local ethical committee.

### 2.2. Radiopharmaceutical and SPECT

The SPECT equipment employed in this study (CERASPECT, Digital Scintigraphics, Waltham, MA) acquires brain perfusion images of $^{99m}$Tc-hexamethylpropylene amine oxime (HMPAO) by a camera equipped with a stationary NaI(Tl) annular crystal and an array of 63 photomultipliers built outside the crystal. The cylindrical-shaped, low-energy, high-resolution lead collimator is the only moving piece during the acquisition at 15 s/stop over 120 stops, with the head of the patient positioned inside. In this way the system optimizes the trade-off between spatial resolution and counting statistics. Sensitivity of the collimator with a point source in air is 190 cps/MBq (7.0 cps/∝Ci), with a spatial resolution for the 140 KeV of 99mTc<8.5 mm at the centre of rotation and 6.3 mm in peripheral regions (full width-half maximum). Geometry of the holes built in the collimator is equivalent to a three-head rotating gamma-camera, in that three different regions of the detecting crystal contribute to acquisition of counts during each angular position. Dedicated hardware and software procedures average these three different sinograms into sinograms equivalent to those generated by a three-head camera (Genna and Smith, 1988).

All SPECT acquisitions were performed 45–90 min after the i.v. injection of 800 to 1000 MBq of freshly prepared $^{99m}$Tc-HMPAO ($^{99m}$Tc-HMPAO, Ceretec®, Amersham International plc, Little Chalfont, UK). Sensory input was minimized whilst injecting the tracer in a quiet, dimly lit room, with the patient lying on a reclining chair (eyes closed and ears unplugged). Sixty-four axial slices parallel to the bicommissural (AC-PC) line, 1.67 mm thick, were reconstructed on a 128 × 128 matrix (1 pixel = 1.67 mm) using a 2-d Butterworth filtered backprojection (cut-off 1 cm, order 10). The reconstructed images were corrected for attenuation with Chang's first-order method, applying an attenuation coefficient equal to 0.11/cm (18) (Chang, 1978).

### 2.3. Standardisation software and statistical analyses

#### 2.3.1. CBA

CBA (Applied Medical Imaging©, Uppsala, Sweden) is a software tool for analysis of neuroimaging data (Greitz et al., 1991). All image sets were spatially normalized into the stereotactic space of the atlas by using the global polynomial transformation (Thurfjell et al., 1995). It consists of translations, rotations and linear scaling along and around each of the three image axes. The system also contains 18 nonlinear shape-deforming parameters, which makes it possible to individualize the shape of the brain. In this study, a fully automatic method was used in which all scans were registered with a SPECT template (Andersson and Thurfjell, 1997).

For evaluation and statistical analysis of the reformatted data sets, 27 VOIs were selected in each hemisphere, in order to cover most of the cortical and subcortical brain structures possibly involved in AD on the basis of the current literature (Poulin and Zakzanis, 2002; Van Heertum and Tikofsky, 2003). These regions corresponded to Brodmann areas (BAs) and numeration in prefrontal (BA9, BA10, BA46), frontal (BA4, BA6, BA8, BA44, BA45), parietal (BASE = BA1 + 2 + 3, BA5, BA7, BA39, BA40) and temporal (BA21, BA37, BA38, hippocampus) cortex. Four regions, representing primary and associative auditory cortex (AUD = BA22 + 41 + 42 + 52), were merged into one single VOI. The remaining regions corresponded to cingulate (BA24, BA31, BA32) and occipital (BA17, BA18, BA19) cortex as well as deep grey structures (nc. caudatus, putamen and thalamus). In order to obtain a set of normalized relative flow data, a scaling factor was computed averaging all brain voxels data and setting the global brain average to a pre-defined value. The normalized value was set to 50 "uptake units," and all rCBF values were related to this value.

#### 2.3.2. Statistical analysis

After adaptation and definitions of VOIs using CBA, the $^{99m}$Tc-HMPAO uptake data of all subjects were exported to a statistical package (Systat 10, 2000) for subsequent statistical analysis. CBF data were submitted to analysis of variance (ANOVA) in two steps: the first by considering only individual VOIs and the second by using the principal components as identified by PCA. Since there were age group differences, we used ANCOVA (analysis of covariance) instead of ANOVA.

PCA was performed on all 94 subjects and was based on all 54 VOIs (27 for each hemisphere). PCA is a data-driven technique (i.e., there is no a-priori model or hypothesis) that transforms a number of correlated variables by clustering them into common factors, such that variables with higher loadings within each factor are highly correlated, but factors are uncorrelated. Variables are summarized in a few dimensions while retaining most of the information. Each factor, or principal component (PC), explains a different part of the total variance of data set.

Principal components may be treated as new variables and their values computed for each case. These values are known as factor scores or component scores (CS) and are a linear combination of each variable included in the analysis. They should be used both to re-evaluate group differences and as predictor variables in diagnostic research. However, in the latter case, it is preferable not to use CS, but an imperfect estimate (coarse component scores, CCS) generated by summing all the VOIs with higher loading in a given factor. An advantage to using CCS is that they can more easily be computed and interpreted than CS and can also be compared between studies (Pett et al., 2003). The number of factors was determined by the number of eigenvalues greater than one. Variables that had an absolute factor loading greater than 0.5 were regarded as representative of the factor. This value is purely arbitrary, but it is commonly used since it explains a moderate part of the variance of the factor. By increasing the value further, some variables should be eliminated from the calculation of CCS reducing the variance explained by these scores. Furthermore CCS are computed only from VOI with higher

loadings on each PC and each VOI is entered only one time in PC calculation. Stability of the PCA was evaluated with the T2 Hotelling test.

ANCOVA was applied to VOI values and then to CCS of PCs to test for statistical significance of CBF differences, considering groups as a between-subject variable. As for VOI analysis, a third within-factor variable was considered, i.e. the hemisphere. The significance level for all analyses was set to $P \leq 0.05$.

Discriminant analysis (DA) was also performed to estimate the relationship between groupings performed according to the clinical diagnosis and SPECT data. DA was limited to CCS since a relevant problem of multicollinearity (a condition in which a set of predictor variables are highly correlated among themselves) was present with VOIs. A way to handle the problem of multicollinearity is by first conducting a PCA and then doing a discriminant function analysis on the component scores. Since the interest was in the correct classification of both modAD and mildAD, DA was performed considering all three groups. The outcome of DA resulted in two discriminant functions (DF). DF are linear combination of variables included in the analysis and their importance is given by the total variance explained by each function. Significance of DA was tested by means of the 'approx. *F* value'.

## 3. Results

In the VOI analysis, there was a significant interaction between VOIs and Groups ($F(52,2262) = 4.825$; $P<0.001$). No hemispheric effect was found. The ANCOVA performed on the average value of bilateral VOIs found in both comparisons (i.e., CTR vs. mildAD and CTR vs. modAD) six bilateral Brodmann areas (BAs, 21, 37, 38, 39, 31 and nc. caudatus) belonging to temporal, parietal and limbic cortex and to the deep grey structures in which patients showed a significant rCBF decrease as compared with normal controls. Four other VOIs showed a significant rCBF distribution decrease in only one comparison. (BAs AUD, 19, 40 and hippocampus, see Table S1 and Fig. S1 in supplementary electronic material). Some BAs belonging to the frontal (BAs 4, 6, 24, 32, 46) and parietal (BASE) cortices and the putamen showed significant relative rCBF increases in patients compared with the CTR group.

PCA identified 12 PCs that explained 82% of the total variance. The T2 test showed that there were only two outliers in our patient group ($P<0.01$). The VOIs with the highest factor loading for each PC are shown in Table 1. CCS were computed summing all VOIs with higher factor loading of each PC and then standardizing raw data on a 0–1 scale. In the overall analysis there was a PC*group interaction ($F(22,957) = 4.515$, $P<0.001$). In the CTR vs. mildAD comparison in four PCs that included mainly VOIs of bilateral temporo-parietal-cingulate regions, there was a significant rCBF distribution decrease (PC2, PC7, PC8 and PC11; Table 1, Fig. 1). The same PCs showed significant differences in the CTR vs. modAD comparison with the addition of PC9, which included the hippocampi bilaterally (Table 1, Fig. 2).

As reported in Table 1, PCA seems to group VOIs according to physiology (i.e. PC1: bilateral pre-motor, motor and somato-sensory cortex; PC5: bilateral visual and visual association cortex) or to anatomy (i.e. PC6: bilateral central structures; PC9: bilateral hippocampi; PC10 and PC12: left and right, respectively, dorso-lateral frontal cortex and some adjacent VOIs). Three PCs, PC2 (left parietal cortex), PC7 (right temporo-occipital cortex) and PC8 (left temporal cortex), included lateralised adjacent VOIs and showed clear density distribution differences among groups (Fig. 3). These PCs were not correlated with age.

The two DF obtained using all CCS values significantly discriminated the groups (approx. $F(24,160) = 6,42$, $P<0.001$). The percentage of subjects correctly classified was 95, 70, and 81 for CTR, mildAD and modAD, respectively. However, when patients were considered together, the misclassifications decreased to 13.3% for mildAD and to 7.4% for modAD (Table 2). To further investigate how each DF differentiated within the three groups, discriminant scores for DF1 against DF2 were plotted (Fig. 4). DF1 centroid values for CTR, mildAD and modAD were respectively −1.508, 0.764 and 1.219, whereas DF2 centroid values were 0.125, −0.925, and 0.856. Centroid analysis indicated that DF1, which explained 75.6% of total dispersion, effectively discriminated between each of the three groups, whereas DF2, which explained the remaining 24.4%, was more effective in discriminating mildAD from modAD. The PC with the largest coefficients in DF1 was PC2, while for DF2 it was PC8.

## 4. Discussion

### 4.1. Interpretation of the findings

The main finding of the study was the identification by PCA of large regions in which perfusion significantly decreased in mildAD as compared with controls, i.e., the real clinical question in early diagnosis. In fact, in the CTR vs. mildAD comparison, the significant areas highlighted by CBA-PCA-ANCOVA disclosed in mildAD a significantly lower rCBF distribution in large regions in both hemispheres (i.e. temporal lobe, inferior parietal lobe, precuneus and posterior cingulate cortex; see Fig. 1).

The grouping of some regions in principal components seemed to be based either on their anatomo-functional proximity or on cytoarchitectonic similarity. As an example, it is worth noting that PC1, PC4, PC5 and PC6 grouped bilateral regions that belonged to well-defined cerebral areas, namely brain vertex, prefrontal cortex, visual cortex and deep grey structures, respectively. Moreover, the regions known to be affected by AD neurodegeneration were grouped together in five PCs. This is the case for PC7 and PC8, in which left temporal cortex along with parietal cortex and right temporal cortex, respectively, belonged to the same principal component. This was also true for PC2 and PC9 in which left parieto-cingulate cortex and both

**Table 1**
CCS mean and S.D. for each PC and group. Significant decreases on analysis of covariance are reported for CTR vs. mildAD and CTR vs. modAD comparisons.

| PC | VOI with high loadings on the PC | Group | | | | | | Group effect | | CTR vs MildAD | | CTR vs ModAD | |
|---|---|---|---|---|---|---|---|---|---|---|---|---|---|
| | | CTR | | MildAD | | ModAD | | $F(2,90)$ | $P\leq$ | $F(1,64)$ | $P\leq$ | $F(1,61)$ | $P\leq$ |
| | | Means | S.D. | Means | S.D. | Means | S.D. | | | | | | |
| PC1 | BA04R,BA04L,BA05R,BA06R,BA06L,BA07R,BA08R,BASER,BASEL | 0.57 | 0.11 | 0.64 | 0.20 | 0.66 | 0.11 | | | | | | |
| PC2 | BA05L,BA07L,BA31R,BA31L,BA39L,BA40L | 0.77 | 0.09 | 0.61 | 0.26 | 0.59 | 0.22 | 10.877 | 0.000 | 14.106 | 0.000 | 16.380 | 0.000 |
| PC3 | BA24R,BA24L,BA32R,BA32L | 0.62 | 0.12 | 0.65 | 0.13 | 0.55 | 0.18 | 4.968 | 0.009 | 10.164 | 0.002 | | |
| PC4 | BA09R,BA09L,BA10R,BA10L,BA46R,BA46L | 0.63 | 0.11 | 0.61 | 0.17 | 0.72 | 0.15 | | | | | | |
| PC5 | BA17R,BA17L,BA18R,BA18L,BA19L | 0.57 | 0.15 | 0.51 | 0.19 | 0.58 | 0.28 | | | | | | |
| PC6 | CDR,CDL,PTR,THR,THL | 0.72 | 0.13 | 0.60 | 0.21 | 0.68 | 0.18 | | | | | | |
| PC7 | BA19R,BA21R,BA37R,BA39R | 0.68 | 0.12 | 0.55 | 0.18 | 0.54 | 0.22 | 8.921 | 0.000 | 14.085 | 0.000 | 14.975 | 0.000 |
| PC8 | AUDR,BA21L,BA37L,BA38L | 0.77 | 0.08 | 0.63 | 0.18 | 0.74 | 0.16 | 12.084 | 0.000 | 25.335 | 0.000 | 4.575 | 0.036 |
| PC9 | HPR,HPL | 0.66 | 0.16 | 0.54 | 0.21 | 0.49 | 0.13 | 3.400 | 0.038 | | | 11.227 | 0.001 |
| PC10 | AUDL,BA44L,BA45L | 0.49 | 0.17 | 0.45 | 0.25 | 0.44 | 0.17 | | | | | | |
| PC11 | BA38R,PTL | 0.42 | 0.14 | 0.32 | 0.14 | 0.33 | 0.18 | 3.937 | 0.023 | 7.601 | 0.008 | 6.033 | 0.017 |
| PC12 | BA40R,BA44R,BA45R | 0.35 | 0.16 | 0.35 | 0.22 | 0.40 | 0.17 | | | | | | |

BA = Brodmann's area; AUD = BA22 + 41 + 42, + 52; CD = nc. Caudatus; TH = thalamus; BASE = BA 1 + 2 + 3; PT = putamen; HP = hippocampus; R = right; L = left. The CCS values are standardised to a 0–1 scale.

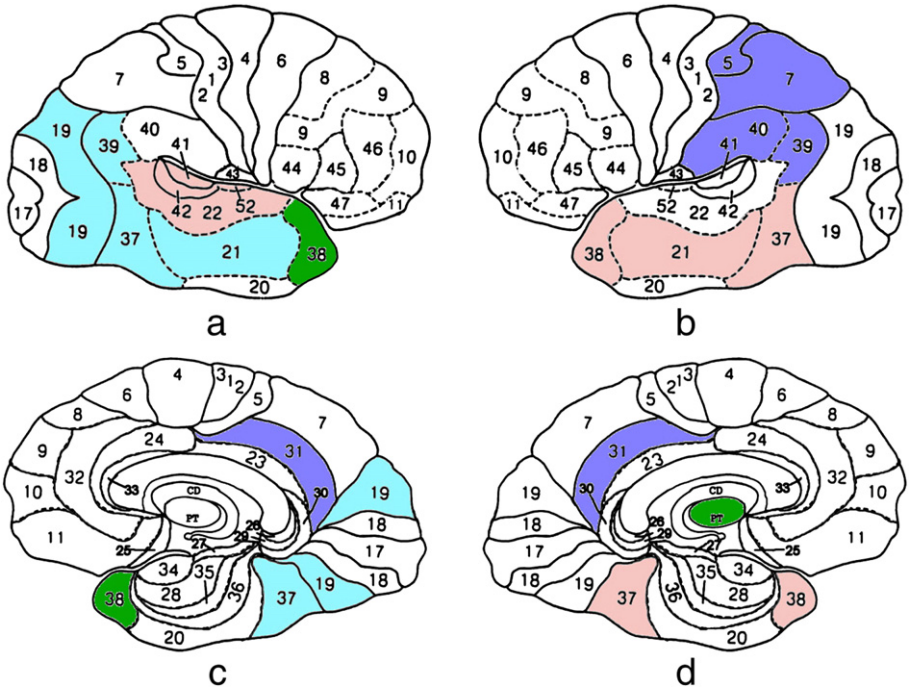


**Fig. 1.** Representation of lateral and medial aspects of hemispheres depicting the four factors (PCs 2, 7, 8 and 11) in which CCS in mildAD was significantly decreased compared with CCS in the CTR. a = right lateral aspect; b = left lateral aspect; c = right medial aspect; d = left medial aspect. PC2 = blu, PC7 = cyan, PC8 = dark salmon, PC11 = green.

hippocampi, respectively, were grouped together. In fact, the precuneus and the posterior cingulate cortex have been shown to be probably the first regions to be affected by hypoperfusion/hypometabolism, both in AD (Minoshima et al., 1997; Kerrouche et al., 2006) and in mild cognitive impairment (Chételat et al., 2003; Borroni et al., 2006). This was also strengthened by the finding that PC2 proved to be the variable that best discriminated patients from controls, underscoring the role of this region in the disease.

The brain regions showing perfusion defects in mildAD and modAD as compared with CTR matched those previously described in a number of articles (Devous, 2002; Goethals et al., 2002; Dougall et al., 2004 for review). In keeping with a previous study (Kogure et al., 2000), hippocampal perfusion (PC9) was impaired only in modAD and this has previously been related to a discordance between functional and morphological findings with an early compensatory neural plasticity (Matsuda et al., 2002). Left parietal associative cortex

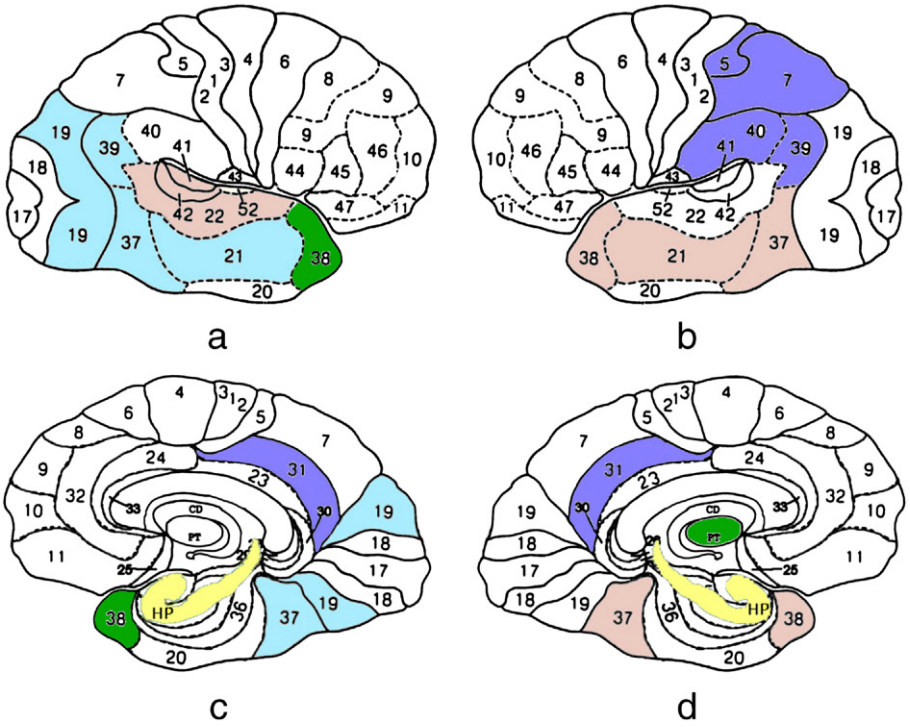


**Fig. 2.** Representation of lateral and medial aspects of hemispheres depicting the five factors (PCs 2, 7, 8, 9 and 11) in which CCS in modAD was significantly decreased compared with CCS in the CTR. a = right lateral aspect; b = left lateral aspect; c = right medial aspect; d = left medial aspect. PC2 = blu, PC7 = cyan, PC8 = dark salmon, PC9 = yellow, PC11 = green.

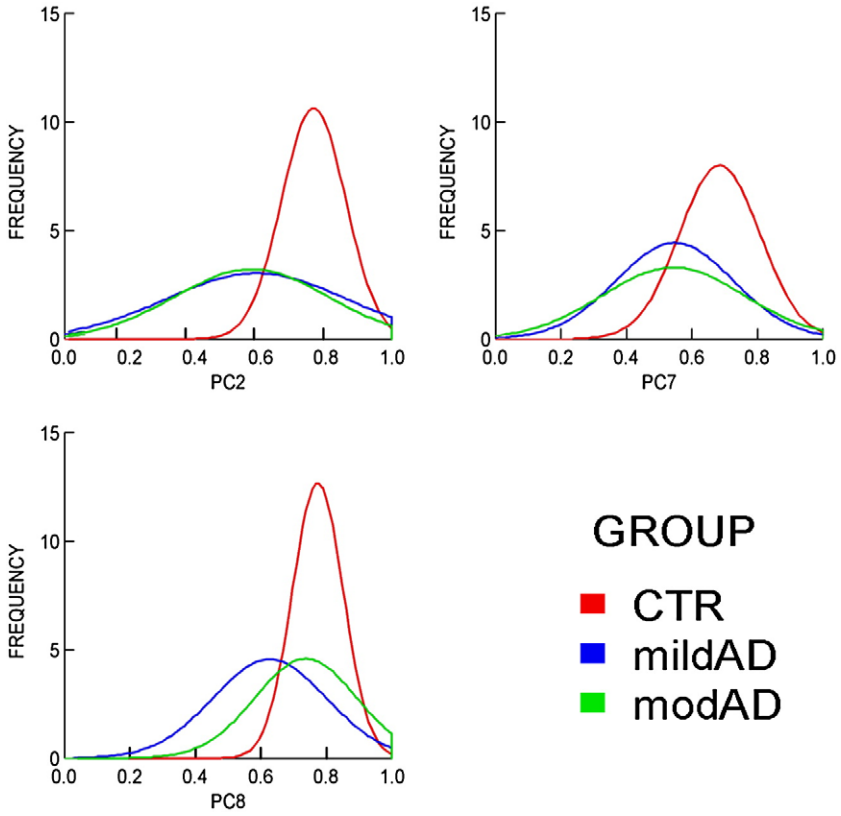


**Fig. 3.** Density distribution (normal curves) for three lateralized PCs. PC2 (top left), PC7 (top right); PC8 (bottom left). On the ordinate is depicted the number of subjects, on the abscissa the CCS values.

(inferior parietal lobe: BAs 39 and 40) perfusion was significantly decreased in both VOI analyses and PCA (PC2, PC7). The grouping of brain regions known to show pathological changes in AD but including only the left or right side (PC2, PC7 and PC8) might be related to the peculiarities of this patient sample, which showed asymmetric defects, as often happens in mild and moderate stages of AD. Fig. 3 illustrates clearly for such PCs differences among groups, as confirmed by ANCOVA, underscoring the discriminative value of VOI clustering. It is worth noting that these PCs were not correlated with the age of the subjects.

The bilateral posterior cingulate covaried in PC2 with large regions of the left lateral parietal lobe. This is consistent with a resting-state rCBF study by PET in AD patients showing a pattern of covariance of the posterior cingulate with the inferior parietal lobe and the supramarginal gyrus (Scarmeas et al., 2004). The posterior cingulate seems to have a central role in the covariance patterns of AD. By $^{18}$F-FDG PET, Salmon et al. (2009) have recently shown that the posterior cingulate was present in the three main PCs, thus covarying with the lateral parietal and temporal cortex, with the anterior cingulate and hippocampal structures, or with precuneus and dorsolateral frontal cortex. These authors commented on the disappearance of a 'default mode' network of brain functioning in the 'resting state' compared with brain activation (Raichle et al., 2001). Activity in this default network would comprise medial cortical structures, including the medial temporal lobe, and lateral associative cortices, and was shown to be reduced in AD patients (Greicius et al., 2004). In fact, multivariate analyses on the default mode network (Greicius et al., 2004) or on resting brain activity (Sackeim et al., 1993) showed a decrease of covariance between frontal and posterior brain regions in AD as compared with healthy controls. Our findings seem in keeping with these data because composition of statistically significant PCs only includes posterior associative areas, without any frontal region covarying in the same PC.

Another point of discussion is the inclusion of bilateral hippocampi in the same PC (PC9) and of bilateral posterior cingulate in the same PC (PC2). These were the only cases of bilateral representation in the same PC among the five significant PCs. In fact, all other left and right regions were represented in different PCs, mainly according to laterality (left side for PC2 and PC8; right side for PC7). As a hypothesis, these findings may indicate the prevalence of neurodegenerative

**Table 2**
Classification matrix obtained by DA considering the 3 groups and the CCS data.

| Clinically assessed group membership | | Predicted group membership | | | | % correct | Patients correctly classified (%) |
|---|---|---|---|---|---|---|---|
| | | *n* | Controls/ CTR | Patients/ mildAD | Patients/ modAD | | |
| Controls | CTR | 37 | 35 | 1 | 1 | 95 | |
| Patients | mildAD | 30 | 4 | 21 | 5 | 70 | 86.7 |
| | modAD | 27 | 2 | 3 | 22 | 81 | 92.6 |
| | Total | | 41 | 25 | 28 | 83 | |

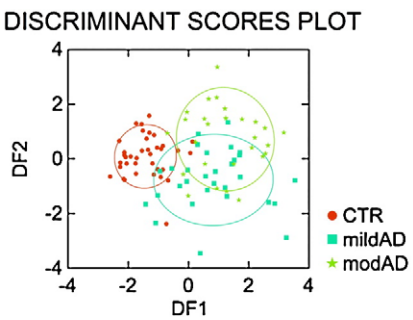


**Fig. 4.** Individual discriminant scores, derived from CCS data, for Discriminant Function 1 (DF1) plotted against those of Discriminant Function 2 (DF2).

changes in hippocampi and posterior cingulate that more directly express anatomic disease severity and thus involve both sides. On the contrary, they may indicate the prevalence of functional disconnection between homologous regions in the two hemispheres, via both intracortical and callosal projections. This interpretation would be consistent with a recent study employing diffusion tensor imaging MRI showing a reduced integrity of intracortical projecting fiber tracts in AD, including corpus callosum, cingulum and fornix, and frontal, temporal and occipital lobe white matter areas (Teipel et al., 2007).

However, VOI analysis did not show a Group*VOI*Hemispheres interaction and thus did not stress any hemispheric laterality due to the disease. In this respect, PCA revealed information not present on VOI analysis by highlighting asymmetries of PCs. Some VOIs, mainly in the frontal and parietal sensori-motor cortex and the putamen, showed a relative rCBF increase as a likely consequence of the semi-quantitative methodology. In such a procedure, the whole brain CBF is normalised to 50; hence, when a patient has large regions with decreased rCBF, some other regions can show a relative increase.

Principal component solutions should be evaluated not only according to empirical criteria but also according to the criterion of "theoretical meaningfulness". Primary and associative visual cortex (PC5), anterior cingulate cortex bilaterally (PC3) and posterior left prefrontal cortex and Broca area (PC10) seemed to be independent of any methodological influence related to either the camera geometry or attenuation correction and strongly suggest a form of either functional connectivity or cytoarchitectonic similarity between the regions present in each principal component. As for the specificity of PC grouping in AD patients, some considerations can be put forward. For instance, it is worth noting that BAs 21, 37 and 38 are largely involved in language comprehension and elaboration in the left hemisphere. This is commonly reflected by cognitive deficit entailing language function, such as verbal memory and categorical verbal fluency, which are indeed found early in AD. On the other hand, in the right hemisphere BAs 21 and 37 were grouped together with BAs 19 and 39, thus especially pointing to the deficit in visuo-spatial function and to constructional apraxia. This is reflected by early deficits in spatial organization, orientation and shape recognition which are often expressed by an impaired performance in visuoconstructional tasks in AD patients.

As for DA, DF2 showed PC8 to be the variable better discriminating the two groups of patients. This finding is likely to be related to the advancing severity disease, since the left temporal lobe is one of the most involved regions in untreated AD patients followed up over time (Nobili et al., 2002). DA was fairly effective in discriminating the three groups under study and the accuracy of the method for normal subjects (95%) was superior to that obtained for patients (70% and 81% for mildAD and modAD, respectively). However, considering as errors only the patients assigned to the control group, we found a sensitivity of 86.7% and 92.6% for mildAD and modAD, respectively. This low percentage of false negatives confirms the usefulness of the PCA in identifying AD patients. Furthermore, according to accurate meta-analyses (Jobst et al., 1998; Dougall et al., 2004), the sensitivity of $^{99m}$Tc-HMPAO SPECT in AD using voxel-based and visual interpretation was about 75%. A recent study (Kerrouche et al., 2006) analysing PET data by PCA has reported a sensitivity of 72% in separating AD from controls. In this respect, the sensitivity of 86.7% and 92.6% found in our study, for mildAD and modAD, respectively, using PCs can be regarded as a considerable improvement adding further value to the analysis. The fact that the PCs with the largest coefficients were PC2 in DF1 and PC8 in DF2 indirectly confirms the reliability of ANCOVA analysis on PCs.

### 4.2. Methodological issues

The statistical approach utilized in this study introduces regional analyses based on the assumption that correlated patterns may exist in normal brain, as well as in AD, among different brain regions and that such relationships may affect rCBF distribution. In this respect, the highly structured connections present in brain physiology and pathology may be described in functional neuroimaging by a careful analysis of the patterns of covariance of rCBF data among VOIs. By using CBA/PCA/ANCOVA, we investigated group differences basing our analysis on coordinated networks instead of independent VOIs or clusters of voxels. Such methods have already been shown to highlight systematic group differences in regional correlations (Moeller et al., 1999; Strother et al., 1993).

One critical point of PCA is how the final solution is influenced by the proportion between the number of subjects and the number of investigated variables. Our choice of an overall PCA was determined by the high number of chosen regions, covering all brain areas potentially involved in mild and modAD. We cannot rule out the hypothesis that including more subjects in the analysis and/or including patients with other diseases might have resulted in different groupings of the VOIs in the PCs. This was the case of a group of normal individuals (Pagani et al., 2002) and of depressed patients (Pagani et al., 2004), in which VOI analysis resulted in a VOI grouping different from the one reported in the present study. Although the impact on the results of the different number of subjects cannot be excluded, such differences could also be due to the peculiar changes in brain networking caused by the specific patho-physiologies. However in all studies PCA increased the depth of the analysis, yielding more information on the processes underlying perfusion distribution measurements.

## 5. Conclusions

In conclusion, the present investigation confirmed the rCBF decrease in several cortical areas in two groups of AD patients, as already widely known in literature. The implementation of principal component analysis revealed a strong covariance between regions belonging to the temporo-parietal cortex and to the limbic system. These finding add depth to the statistical analysis and yield more complete information on the networking underlying pathological changes in AD. Moreover, highlighting functional connectivity points to an alternative approach in group analysis of neuroimaging data.

#### Acknowledgments

The authors thank Dr. Antonietta Di Salvatore for her wise suggestions on statistical methodology and Ms Charlotte Williams for her help in English language revision. The experiments comply with the current laws of the country in which they were performed.

## Appendix A. Supplementary data

Supplementary data associated with this article can be found, in the online version, at doi:10.1016/j.pscychresns.2008.07.016.

## References

Andersson, J.L.R., Thurfjell, L., 1997. Implementation and validation of a fully automatic system for intra- and inter-individual registration of PET brain scans. Journal of Computer Assisted Tomography 21, 136–144.

Bartenstein, P., Minoshima, S., Hirsch, C., Buch, K., Willoch, F., Mösch, D., Schad, D., Schwaiger, M., Kurz, A., 1997. Quantitative assessment of cerebral blood flow in patients with Alzheimer's disease by SPECT. Journal of Nuclear Medicine 38, 1095–1101.

Bonte, F.J., Weiner, M.F., Bigio, E.H., White, C.L., 1997. Brain blood flow in the dementias, SPECT with histopathologic correlation in 54 patients. Radiology 202, 793–797.

Borroni, B., Anchisi, D., Paghera, B., Vicini, B., Kerrouche, N., Garibotto, V., Terzi, A., Vignolo, L.A., Di Luca, M., Giubbini, R., Padovani, A., Perani, D., 2006. Combined 99mTc-ECD SPECT and neuropsychological studies in MCI for the assessment of conversion to AD. Neurobiology of Aging 27, 24–31.

Chang, L.T., 1978. A method for attenuation correction in radionuclide computed tomography. IEEE Transactions on Nuclear Science 25, 638–643.

Chételat, G., Desgranges, B., de la Sayette, V., Viader, F., Eustache, F., Baron, J.C., 2003. Mild cognitive impairment. Can FDG-PET predict who is to rapidly convert to Alzheimer's disease? Neurology 60, 1374–1377.

Devanand, D.P., Habeck, C.G., Tabert, M.H., Scarmeas, N., Pelton, G.H., Moeller, J.R., Mensh, B.D., Tarabula, T., Van Heertum, R.L., Stern, Y., 2006. PET network abnormalities and cognitive decline in patients with mild cognitive impairment. Neuropsychopharmacology 31, 1327–1334.

Devous Sr., M.D., 2002. Functional brain imaging in the dementias: role in early detection, differential diagnosis, and longitudinal studies. European Journal of Nuclear Medicine and Molecular Imaging 29, 1685–1687.
Dougall, N.J., Bruggink, S., Ebmeier, K.P., 2004. Systematic review of the diagnostic accuracy of 99mTc-HMPAO-SPECT in Dementia. American Journal of Geriatric Psychiatry 12, 554–570.
Eidelberg, D., Moeller, J.R., Dhawan, V., Sidtis, J.J., Ginos, J.Z., Strother, S.C., Cedarbaum, J., Greene, P., Fahn, S., Rottenberg, D.A., 1990. The metabolic anatomy of Parkinson's disease: complementary (18F)fluorodeoxyglucose and (18F)fluorodopa positron emission tomographic studies. Movement Disorders 5, 203–213.
Eidelberg, D., Moeller, J.R., Dhawan, V., Spetsieris, P., Takikawa, S., Ishikawa, T., Chaly, T., Robeson, W., Margouleff, D., Przedborski, S., 1994. The metabolic topography of parkinsonism. Journal of Cerebral Blood Flow and Metabolism 14, 783–801.
Folstein, M.F., Folstein, S.E., McHugh, P.R., 1975. "Mini-mental state". A practical method for grading the cognitive state of patients for the clinician. Journal of Psychiatric Research 12, 189–198.
Friston, K.J., Frith, P.F., Frackowiak, S.J., 1993. Functional connectivity: the principal-component analysis of large (PET) data set. Journal of Cerebral Blood Flow and Metabolism 13, 5–14.
Friston, K.J., Holmes, A.P., Worsley, K.J., Poline, J.P., Frith, C.D., Frackowiak, R.S.J., 1995. Statistical parametric maps in functional imaging: a general linear approach. Human Brain Mapping 2, 189–210.
Friston, K., Phillips, J., Chawla, D., Buchel, C., 1999. Revealing interactions among brain systems with nonlinear PCA. Human Brain Mapping 8, 92–97.
Genna, S., Smith, A.P., 1988. The development of ASPECT, an annular single crystal brain camera for high efficiency SPECT. IEEE Transactions on Nuclear Science 35, 654–658.
Goethals, I., Van De Wiele, C., Slosman, D., Dierckx, R., 2002. Brain SPET perfusion in early Alzheimer's disease: where to look? European Journal of Nuclear Medicine and Molecular Imaging 29, 975–978.
Greicius, M.D., Srivastava, G., Reiss, A.L., Menon, V., 2004. Default-mode network activity distinguishes Alzheimer's disease from healthy aging: evidence from functional MRI. Proceedings of the National Academy of Sciences of the United States of America 101, 4637–4642.
Greitz, T., Bohm, C., Holte, S., Eriksson, L., 1991. A computerized brain atlas: construction, anatomical content, and some applications. Journal of Computer Assisted Tomography 15, 26–38.
Habeck, C., Krakauer, J.W., Ghez, C., Sackeim, H.A., Eidelberg, D., Stern, Y., Moeller, J.R., 2005. A new approach to spatial covariance modeling of functional brain imaging data: ordinal trend analysis. Neural Computation 17, 1602–1645.
Hirsch, C., Bartenstein, P., Minoshima, S., Mösch, D., Willoch, F., Buch, K., Schad, D., Schwaiger, M., Kurz, A., 1997. Reduction of regional cerebral blood flow and cognitive impairment in patients with Alzheimer's disease: evaluation of an observer-independent analytic approach. Dementia and Geriatric Cognitive Disorders 8, 98–104.
Houston, A.S., Kemp, P.M., Macleod, M.A., Francis, T.J.R., Colohan, H.A., Matthews, H.P., 1998. Use of significance image to determine patterns of cortical blood flow abnormality in pathological and at-risk Groups. Journal of Nuclear Medicine 39, 425–430.
Hu, D., Yan, L., Liu, Y., Zhou, Z., Friston, K.J., Tan, C., Wu, D., 2005. Unified SPM-ICA for fMRI analysis. Neuroimage 25, 746–755.
Huang, C., Eidelberg, D., Habeck, C., Moeller, J., Svensson, L., Tarabula, T., Julin, P., 2007. Imaging markers of mild cognitive impairment: multivariate analysis of CBF SPECT. Neurobiology of Aging 28, 1062–1069.
Imran, M.B., Kawashima, R., Awata, S., Sato, K., Kinomura, S., Ono, S., Yoshioka, S., Sato, M., Fukada, H., 1999. Parametric mapping of cerebral blood flow deficits in Alzheimer's disease: a SPECT study using HMPAO and image standardization technique. Journal of Nuclear Medicine 40, 244–249.
Jagust, W.J., Eberling, J.L., Reed, B.R., Mathis, C.A., Budinger, T.F., 1997. Clinical studies of cerebral blood flow in Alzheimer's disease. Annals of the New York Academy of Sciences 826, 254–262.
Jagust, W., Thisted, R., Devous, M.D., Van Heertum, R., Mayberg, H., Jobst, K., Smith, A.D., Borys, N., 2001. SPECT perfusion imaging in the diagnosis of Alzheimer's disease. A clinical-pathologic study. Neurology 56, 950–956.
Jobst, K.A., Barnetson, L.P., Shepstone, B.J., 1998. Accurate prediction of histologically confirmed Alzheimer's disease and the differential diagnosis of dementia: the use of NINCDS-ADRDA and DMS-III criteria, SPECT, X-Ray CT and Apo E4 in medial temporal lobe dementias. Oxford project to investigate memory and aging. International Psychogeriatrics 10, 271–302.
Jones, K., Johnson, K.A., Becker, J.A., Spiers, P.A., Albert, M.S., Holman, B.L., 1998. Use of singular value decomposition to characterize age and gender differences in SPECT cerebral perfusion. Journal of Nuclear Medicine 39, 965–973.
Kerrouche, N., Herholz, K., Mielke, R., Holthoff, V., Baron, J.C., 2006. $^{18}$FDG PET in vascular dementia: differentiation from Alzheimer's disease using voxel-based multivariate analysis. Journal of Cerebral Blood Flow and Metabolism 26, 1213–1221.
Kogure, D., Matsuda, H., Ohnishi, T., Asada, T., Uno, M., Kunihiro, T., Nakano, S., Takasaki, M., 2000. Longitudinal evaluation of early Alzheimer's disease using Spect. Journal of Nuclear Medicine 41, 1155–1162.
Lozza, C., Baron, J.C., Eidelberg, D., Mentis, M.J., Carbon, M., Marie, R.M., 2004. Executive processes in Parkinson's disease: FDG-PET and network analysis. Human Brain Mapping 22, 236–245.
Matsuda, H., Kitayama, N., Ohnishi, T., Asada, T., Nakano, S., Sakamoto, S., Imabayashi, E., Katoh, A., 2002. Longitudinal evaluation of both morphologic and functional changes in the same individuals with Alzheimer's disease. Journal of Nuclear Medicine 43, 304–311.
McIntosh, A.R., Bookstein, F.L., Haxby, J.V., Grady, C.L., 1996. Spatial pattern analysis of functional brain images using partial least squares. Neuroimage 3, 143–157.
McKeith, I.G., Perry, E.K., Perry, R.H., 1999. Report of the second dementia with Lewy body international workshop: diagnosis and treatment. Consortium on Dementia with Lewy Bodies. Neurology 53, 902–905.
McKhann, G., Drachman, D., Folstein, M., Katzman, R., Price, D., Stadlan, E.M., 1984. Clinical diagnosis of Alzheimer's disease: report of the NINCDS-ADRDA Work Group under the auspices of Department of Health and Human Services Task Force on Alzheimer's Disease. Neurology 34, 939–944.
Minoshima, S., Giordani, B., Berent, S., Frey, K.A., Foster, N.L., Kuhl, D.E., 1997. Metabolic reduction in the posterior cingulate cortex in very early Alzheimer's Disease. Annals of Neurology 42, 85–94.
Moeller, J.R., Nakamura, T., Mentis, M.J., Dhawan, V., Spetsieres, P., Antonini, A., Missimer, J., Leenders, K.L., Eidelberg, D., 1999. Reproducibility of regional metabolic covariance patterns: comparison of four populations. Journal of Nuclear Medicine 40, 1264–1269.
Moeller, J.R., Strother, S.C., Sidtis, J.J., Rottenberg, D.A., 1987. Scaled subprofile model: a statistical approach to the analysis of functional patterns in positron emission tomographic data. Journal of Cerebral Blood Flow and Metabolism 7, 649–658.
Nobili, F., Vitali, P., Canfora, M., Girtler, N., De Leo, C., Mariani, G., Pupi, A., Rodriguez, G., 2002. Effects of long-term Donepezil therapy on rCBF of Alzheimer's patients. Clinical Neurophysiology 113, 1241–1248.
Pagani, M., Gardner, A., Salmaso, D., Sánchez-Crespo, A., Jonsson, C., Jacobsson, H., Lindberg, G., Wägner, A., Hällström, T., Larsson, S.A., 2004. Principal component and volumes of interest analyses in depressed patients by 99m-Tc-HMPAO SPET — a methodological comparison. European Journal of Nuclear Medicine and Molecular Imaging 31, 995–1004.
Pagani, M., Salmaso, D., Jonsson, C., Hatherly, R., Jacobsson, H., Larsson, S.A., Wägner, A., 2002. Brain regional blood flow as assessed by principal component analysis and 99mTc-HMPAO SPET in healthy subjects at rest — normal distribution and effect of age and gender. European Journal of Nuclear Medicine and Molecular Imaging 29, 67–75.
Pett, M.A., Lackey, N.R., Sullivan, J.J., 2003. Making Sense of Factor Analysis in Health Care Research: A Practical Guide. Sage Publications.
Poulin, P., Zakzanis, K.K., 2002. In vivo neuroanatomy of Alzheimer's disease: evidence from structural and functional brain imaging. Brain and Cognition 49, 220–225.
Raichle, M.E., MacLeod, A.M., Snyder, A.Z., Powers, W.J., Gusnard, D.A., Shulman, G.L., 2001. A default mode of brain function. Proceedings of the National Academy of Sciences of the United States of America 98, 676–682.
Roman, G.C., Tatemichi, T.K., Erkinjuntti, T., Cummings, J.L., Masdeu, J.C., Garcia, J.H., Amaducci, L., Orgogozo, J.M., Brun, A., Hofman, A., 1993. Vascular dementia: diagnostic criteria for research studies. Report of the NINDS-AIREN International Workshop. Neurology 43, 250–260.
Sackeim, H.A., Prohovnik, I., Moeller, J.R., Mayeux, R., Stern, Y., Devanand, D.P., 1993. Regional cerebral blood flow in mood disorders. II. Comparison of major depression and Alzheimer's disease. Journal of Nuclear Medicine 34, 1090–1101.
Salmon, E., Kerrouche, N., Herholz, K., Perani, D., Holthoff, V., Beuthien-Baumann, B., Degueldre, C., Lemaire, C., Luxen, A., Baron, J.C., Collette, F., Garraux, G., 2006. Decomposition of metabolic brain clusters in the frontal variant of frontotemporal dementia. Neuroimage 30, 871–878.
Salmon, E., Kerrouche, N., Perani, D., Lekeu, F., Holthoff, V., Beuthien-Baumann, B., Sorbi, S., Lemaire, C., Collette, F., Herholz, K., 2009. On the multivariate nature of brain metabolic impairment in Alzheimer's disease. Neurobiology of Aging 30, 186–197.
Salmon, E., Sadzot, B., Maquet, P., Degueldre, C., Lemaire, C., Rigo, P., Comar, D., Franck, G., 1994. Differential diagnosis of Alzheimer's disease with PET. Journal of Nuclear Medicine 35, 391–398.
Scarmeas, N., Habeck, C.G., Zarahn, E., Anderson, K.E., Park, A., Hilton, J., Pelton, G.H., Tabert, M.H., Honig, L.S., Moeller, J.R., Devanand, D.P., Stern, Y., 2004. Covariance PET patterns in early Alzheimer's disease and subjects with cognitive impairment but no dementia: utility in group discrimination and correlations with functional performance. Neuroimage 23, 35–45.
Stoub, T.R., deToledo-Morrell, L., Stebbins, G.T., Leurgans, S., Bennett, D.A., Shah, R.C., 2006. Hippocampal disconnection contributes to memory dysfunction in individuals at risk for Alzheimer's disease. Proceedings of the National Academy of Sciences of the United States of America 103, 10041–10045.
Strother, S.C., Anderson, J.R., Schaper, K.A., Sidtis, J.J., Liow, J.S., Woods, R.P., Rottenberg, D.A., 1995. Principal component analysis and the scaled subprofile model compared to intersubject averaging and statistical parametric mapping: I. "Functional connectivity" of the human motor system studied with (15O)water PET. Journal of Cerebral Blood Flow and Metabolism 15, 738–753.
Strother, S.C., Moeller, J.R., Sitidis, J.J., Rottenberg, D.A., 1993. Using principal component analysis to identify a disease independent pattern of cerebral metabolic activation: the reticular activating system? In: Uemura, K., Lassen, N.A., Kanno, I. (Eds.), Quantification of Brain Function. Elsevier Science, Amsterdam, pp. 491–498.
Syed, G.M.S., Eagger, S., O'Brien, J., Barrett, J.J., Levy, R., 1992. Patterns of regional cerebral blood flow in Alzheimer's disease. Nuclear Medicine Communications 13, 656–663.
Systat 10, 2000. Statistics. SPSS.
Teipel, S.J., Stahl, R., Dietrich, O., Schoenberg, S.O., Perneczky, R., Bokde, A.L., Reiser, M.F., Möller, H.J., Hampel, H., 2007. Multivariate network analysis of fiber tract integrity in Alzheimer's disease. Neuroimage 34, 985–995.
The Lund and Manchester Groups, 1994. Clinical and neuropathological criteria for frontotemporal dementia. Journal of Neurology Neurosurgery and Psychiatry 57, 416–418.
Thurfjell, L., Bohm, C., Bengtsson, E., 1995. CBA — an atlas based software tool used to facilitate the interpretation of neuroimaging data. Computer Methods & Programs in Biomedicine 4, 51–71.
Van Heertum, R.L., Tikofsky, R.S., 2003. Positron emission tomography and single-photon emission computed tomography brain imaging in the evaluation of Dementia. Seminars in Nuclear Medicine 33, 77–85.
Worsley, K.J., Marrett, S., Neelin, P., Vandal, A.C., Friston, K.J., Evans, A.C., 1996. A unified statistical approach for determining significant signals in images of cerebral activation. Human Brain Mapping 4, 58–73.
Zuendorf, G., Kerrouche, N., Herholz, K., Baron, J.C., 2003. Efficient principal component analysis for multivariate 3D voxel-based mapping of brain functional imaging data sets as applied to FDG-PET and normal aging. Human Brain Mapping 18, 13–21.

**TABLE 1** supplementary electronic data

**Means and S.D. for each VOI and group. Significant changes at ANCOVA are reported for CTR vs mildAD and CTR vs modAD comparisons.**

| VOIs | Group | | | | | | Group effect | | CTR vs mildAD | | CTR vs modAD | |
|---|---|---|---|---|---|---|---|---|---|---|---|---|
| | CTR | | mildAD | | modAD | | | | | | | |
| | M | S.D. | M | S.D. | M | S.D. | $F(2,90)$ | $P \leq$ | $F(1,64)$ | $P \leq$ | $F(1,61)$ | $P \leq$ |
| AUD | 45.8 | 1.6 | 45.2 | 2.8 | 43.7 | 1.9 | 3.946 | .023 | | | 12.783 | .001 |
| BA04 | 41.5 | 2.3 | 42.9 | 4.5 | 43.9 | 2.3 | 3.557 | .033 | | | 14.970 | .000 |
| BA05 | 46.6 | 2.6 | 46.7 | 4.4 | 46.1 | 3.2 | | | | | | |
| BA06 | 42.7 | 2.1 | 44.5 | 3.5 | 44.9 | 2.2 | 4.781 | .011 | 4.574 | .036 | 14.705 | .000 |
| BA07 | 46.0 | 2.1 | 45.2 | 4.1 | 44.4 | 2.3 | | | | | | |
| BA08 | 42.4 | 2.6 | 42.7 | 4.4 | 44.5 | 2.6 | | | | | | |
| BA09 | 43.3 | 2.2 | 42.8 | 3.6 | 44.6 | 3.2 | | | | | | |
| BA10 | 43.1 | 2.2 | 43.1 | 2.9 | 44.5 | 2.7 | | | | | | |
| BA17 | 53.3 | 2.2 | 53.0 | 2.8 | 53.3 | 4.2 | | | | | | |
| BA18 | 46.5 | 2.3 | 46.0 | 3.0 | 47.1 | 3.6 | | | | | | |
| BA19 | 44.8 | 1.7 | 43.3 | 2.4 | 44.2 | 3.1 | 5.408 | .006 | 11.305 | .001 | | |
| BA21 | 45.0 | 1.8 | 42.0 | 2.8 | 42.9 | 2.2 | 17.002 | .000 | 29.054 | .000 | 24.704 | .000 |
| BA24 | 41.2 | 4.7 | 42.2 | 5.5 | 37.3 | 6.8 | 6.202 | .003 | 6.720 | .012 | | |
| BA31 | 55.5 | 2.1 | 53.3 | 3.4 | 51.8 | 3.6 | 14.841 | .000 | 12.050 | .001 | 23.101 | .000 |
| BA32 | 48.5 | 2.1 | 49.1 | 2.6 | 48.7 | 3.2 | 3.585 | .032 | 11.335 | .001 | | |
| BA37 | 46.6 | 2.2 | 44.1 | 3.3 | 45.3 | 2.5 | 9.487 | .000 | 15.412 | .000 | 9.581 | .003 |
| BA38 | 39.9 | 3.6 | 36.7 | 3.9 | 38.2 | 3.9 | 5.544 | .005 | 11.263 | .001 | 5.366 | .024 |
| BA39 | 44.8 | 1.7 | 42.2 | 2.8 | 42.3 | 2.8 | 16.966 | .000 | 23.885 | .000 | 23.074 | .000 |
| BA40 | 44.1 | 1.7 | 42.0 | 3.0 | 43.8 | 1.7 | 8.384 | .000 | 10.535 | .002 | | |
| BA44 | 45.4 | 2.2 | 45.8 | 2.8 | 46.0 | 2.5 | | | | | | |
| BA45 | 45.9 | 2.1 | 46.4 | 2.8 | 46.5 | 2.1 | | | | | | |
| BA46 | 44.1 | 2.2 | 44.0 | 2.8 | 46.0 | 2.7 | 5.312 | .007 | | | 6.378 | .014 |
| BASE | 41.6 | 1.3 | 42.5 | 2.5 | 42.9 | 1.8 | 4.327 | .016 | | | 13.582 | .000 |
| CD | 46.9 | 3.7 | 43.0 | 5.1 | 44.1 | 5.5 | 4.678 | .012 | 8.702 | .004 | 5.248 | .025 |
| HP | 46.9 | 2.7 | 44.7 | 3.6 | 44.0 | 2.2 | 3.400 | .038 | | | 11.227 | .001 |
| PT | 57.4 | 2.6 | 58.8 | 3.8 | 59.6 | 3.1 | 3.353 | .039 | | | 6.985 | .010 |
| TH | 57.2 | 3.1 | 54.2 | 5.9 | 56.4 | 4.2 | | | | | | |

**BA= Brodmann's area. AUD= BA22+41+42,+52; BASE= BA1+2+3; CD= nc. caudatus; HP=hippocampi; PT=putamen; TH= thalamus.**

**Values are expressed in units normalized to the average of all brain voxels set to 50.**

CLOSE

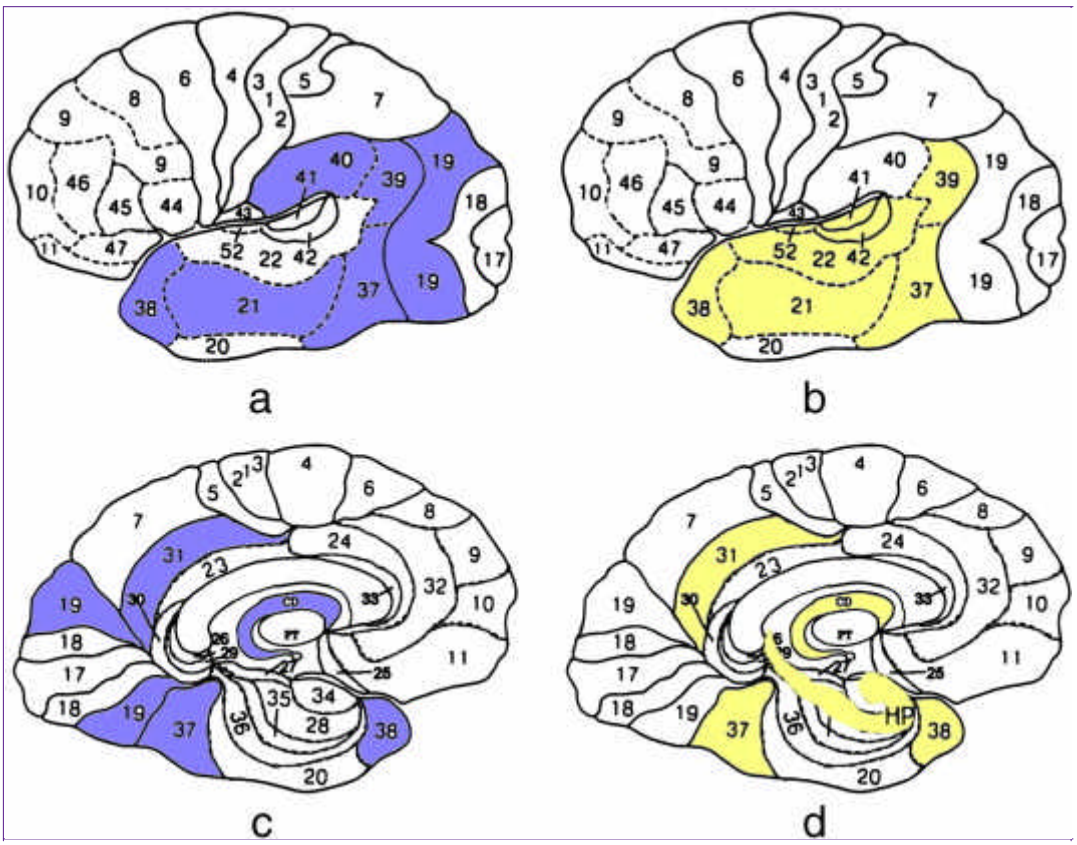


High-quality image (360K)Fig. S1. Representation of lateral and medial aspects of hemispheres depicting VOIs in which rCBF in mildAD and modAD significantly decreased when compared to rCBF in the CTR. VOIs represent the average of left and right values and the choice to project them on the left hemisphere is subjective. a = lateral aspect CTR *minus* mildAD; b = lateral aspect CTR *minus* modAD; c = medial aspect CTR *minus* mildAD; d = medial aspect CTR *minus* modAD.Blu color refers to the CTR-mildAD comparison and yellow to the CTR-modAD one.